EPJ Web of Conferences **380**, 01018 (2026) https://doi.org/10.1051/epjconf/202638001018
ICISCT'25

Circularly polarized antenna with gain enhancement via a single-layer Near-Zero-Index metasurface superstrate

Chaymae Chahboun[1*], *Safia* Jaouad[1], *Fatima Z.* Khoutar[1], *Otman* Mrabet[1], and *Mariem* Aznabet[1]

[1] 1 ISD Laboratory, Faculty of Science, Abdelmalek Essaadi University, Tetouan, Morocco

Abstract. This paper presents a dual-fed square patch antenna loaded with a single-layer near-zero-index metasurface (NZIM) superstrate for circularly polarized operation at 5.8 GHz. The radiating patch is excited by two orthogonal quarter-wave microstrip feed lines, allowing the TM_{10} and TM_{01} modes to be generated simultaneously and used for circular polarization. The proposed superstrate consists of a 9 × 9 array of nested split-ring resonator elements and is placed 26 mm above the patch, which is close to one half of the free-space wavelength at the operating frequency. The effective-parameter retrieval of the unit cell confirms a near-zero refractive index around 5.8 GHz, supporting wave collimation and improving the antenna directivity. Compared with the reference antenna without the metasurface, the proposed structure increases the simulated peak gain from 6.1 dBi to 10.2 dBi and improves the radiation efficiency from 69% to 95%. In addition, the axial ratio decreases from approximately 12 dB to less than 3 dB near resonance, confirming the improvement of circular polarization. These results show that the proposed single-layer NZIM superstrate can be an effective approach for compact antennas requiring higher gain, better radiation efficiency, and more stable polarization performance in 5G, satellite, and IoT applications.

1 Introduction

The rapid evolution of wireless communication technologies has created a growing need for advanced antenna designs that can provide high performance, and adaptability in different operating environments. In this work, an antenna designed to operate at 5.8 GHz is proposed, with particular attention to applications related to the expanding 5G frequency band. The design is based on the integration of a microstrip patch antenna with a metasurface structure in order to support dual-mode polarization and improve the overall antenna performance.

Microstrip patch antennas are commonly used in modern wireless systems because of their compact size, low profile, and ease of integration. However, their limited gain and

[*] Corresponding author: chaymae.chahboun@etu.uae.ac.ma

directionality can make it difficult to satisfy the demanding requirements of 5G communication systems [1–3]. To overcome these limitations, the proposed antenna uses a single square patch radiator excited by two orthogonal quarter-wave microstrip feed lines. This feeding configuration allows the excitation of two orthogonal polarization modes, namely TM_{10} and TM_{01}, which are optimized to operate around the 5.8 GHz frequency band.

In recent years the metasurfaces have gained significant attention owing to their ability to control electromagnetic waves with high precision, offering new possibilities for enhancing antenna performance [4–7]. In the proposed design, the metasurface array performs two main functions. First, it convert the linearly polarized incident waves into circular polarization, for reducing polarization mismatch losses and improving communication efficiency. Second, the metasurface is optimized to increase the antenna gain by controlling the radiation pattern and improving beam direction, making the antenna suitable for 5G applications [8 –13].

The proposed antenna is designed to achieve an axial ratio below 3 dB, confirming good circular polarization with minimal distortion between the two orthogonal field components. This is achieved through the optimization of the antenna structure and the integration of metasurface concepts with conventional microstrip antenna theory.

2 Antenna design and methodology

2.1 Dual-fed square patch antenna

The proposed antenna consists of a square microstrip patch placed below a single-layer NZIM superstrate, as shown in Fig. 1. The patch has dimensions of 18 x 18 mm^2 and is printed on a grounded Rogers RO4003C substrate with a relative permittivity of 3.55 and a thickness of 1.524 mm. The overall size of the lower antenna substrate is 67 x 67 x 1.524 mm^3. Two identical quarter-wave microstrip feeding lines are arranged orthogonally in order to excite the TM10 and TM01 modes around 5.8 GHz. The dual-feed configuration is selected to obtain the amplitude and phase conditions required for circular polarization.

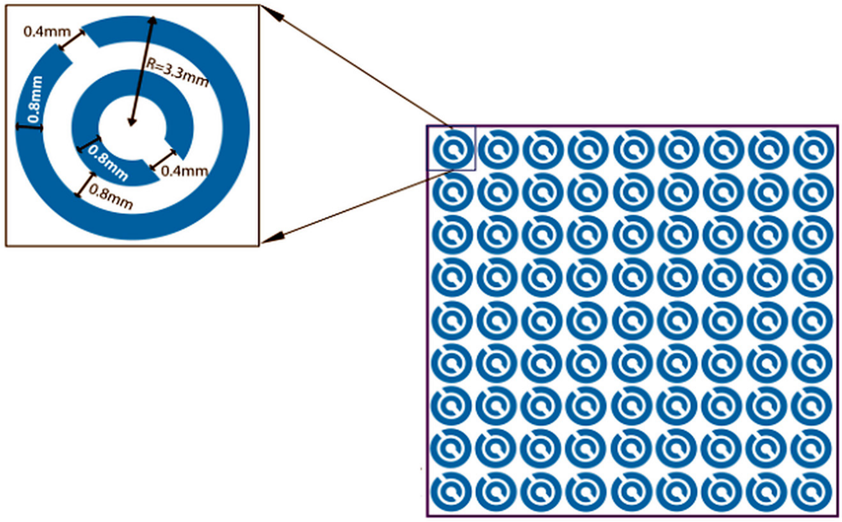

Fig. 1. Top view of the 9 x 9 NZIM metasurface and detailed geometry of the nested split-ring resonator unit cell.

2.2 NZIM metasurface superstrate

The metasurface consists of a 9 × 9 two-dimensional array arranged over an aperture similar to that of the antenna substrate. Each unit cell is formed by nested split-ring resonators, which are designed to resonate in the C-band. In the final configuration, the metasurface is placed 26 mm above the patch, corresponding approximately to $\lambda/2$ at 5.8 GHz. This distance was selected after simulation because it gave the best balance between impedance matching, axial-ratio response, and gain improvement.

To verify the electromagnetic behavior of the designed unit cell, its effective parameters were extracted from the simulated scattering parameters using the S-parameter retrieval method [14]. The real and imaginary parts of the retrieved permittivity, permeability, and refractive index are shown in Fig. 2. Around 5.8 GHz, the refractive index becomes close to zero, which confirms the near-zero-index response of the proposed metasurface. This property helps redirect the fields radiated by the patch toward the broadside direction and explains the improvement in directivity. The observed resonance is also consistent with the expected response of compact split-ring resonator structures used in metamaterial and metasurface designs [15].

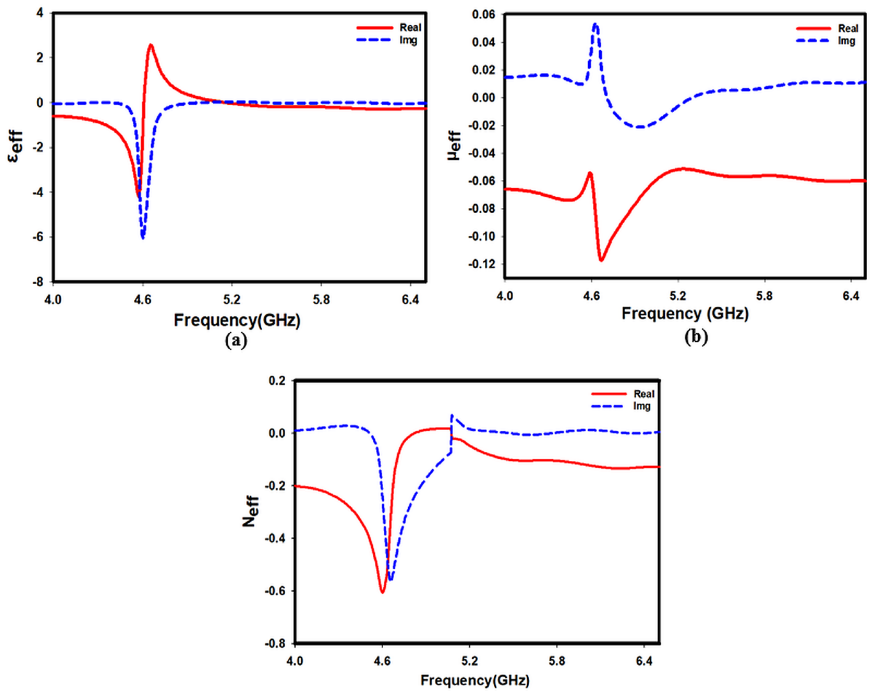

Fig. 2. Retrieved effective parameters of the NZIM unit cell: (a) permittivity, (b) permeability and (c) refractive index.

2.3 Simulation and validation strategy

The complete antenna was optimized using CST Microwave Studio with full-wave three-dimensional electromagnetic simulations. Since the present study is based on numerical results, the credibility of the design is supported by complementary checks. First, the unit-cell response is validated through effective-parameter retrieval. Second, the complete antenna is evaluated against a reference configuration without the metasurface using the same substrate, feeding scheme and numerical conditions. Third, the observed improvements are interpreted through the current distribution and radiation patterns, which verify the physical role of the NZIM superstrate in beam focusing and polarization control.

3 Results and discussion

3.1 Reflection coefficient and inter-port isolation

Fig. 3 compares the simulated S-parameters of the proposed antenna with and without the NZIM superstrate. Both configurations maintain a reflection coefficient below -10 dB around the intended operating frequency. The transmission coefficient between the two feed ports remains lower than -30 dB near 5.8 GHz, indicating good isolation and limited mutual interaction between the orthogonal feeding paths. The metasurface therefore enhances the radiation characteristics without degrading the impedance matching of the dual-fed antenna.

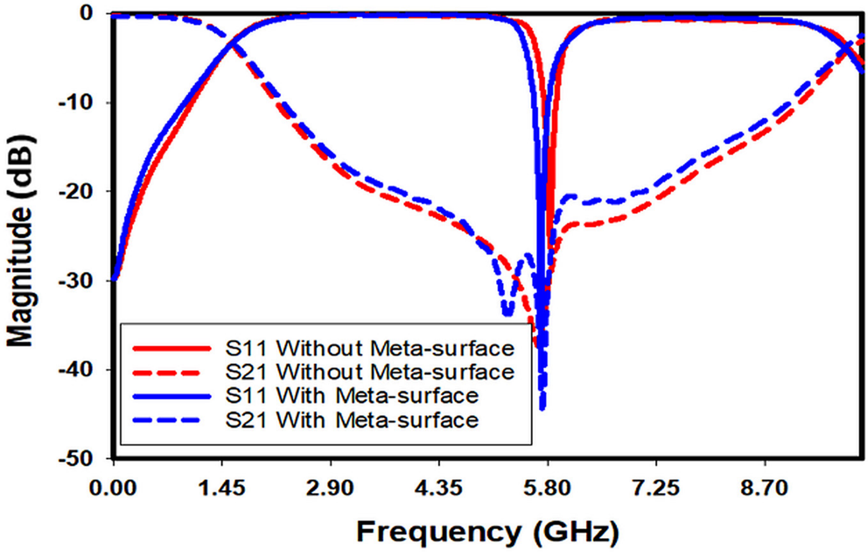

Fig. 3. Simulated S-parameters of the proposed antenna with and without the NZIM metasurface superstrate.

3.2 Surface current distribution

Fig. 4 shows the surface current distribution of the proposed design . The current is mainly limited to the patch and the feed lines and a weak distribution is seen on the rest of the antenna surface in the absence of the metasurface. When the NZIM superstrate is introduced, the stronger currents are observed around the metasurface resonant elements. This shows the interaction between the superstrate and the field radiated by the patch and helps to redistribute the electromagnetic energy over the antenna. The improvement in gain and the more directive radiation pattern obtained with the proposed structure are attributed to the redistribution.

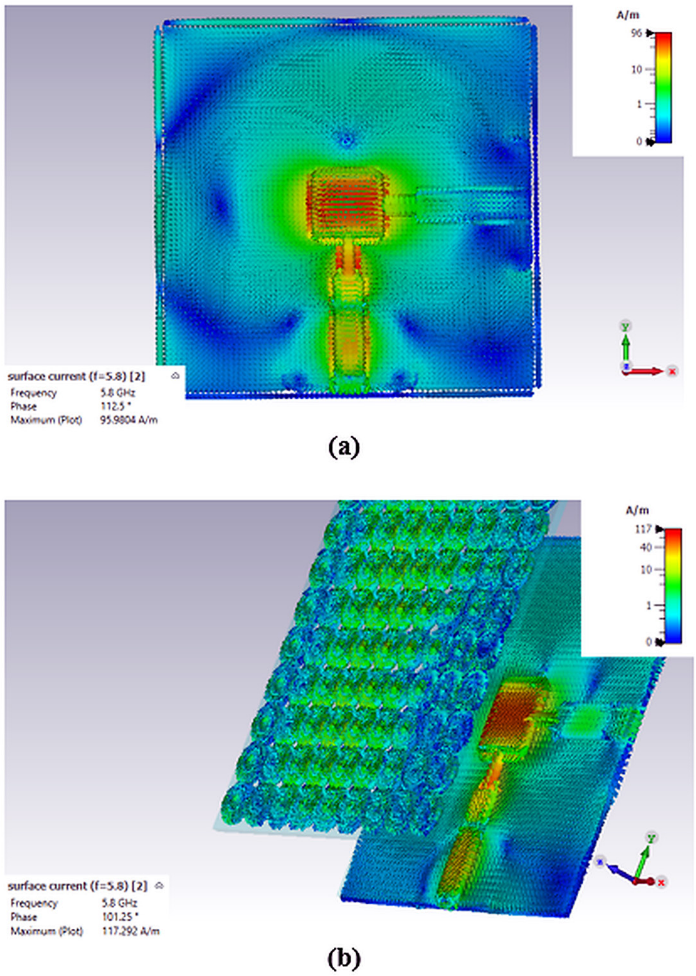

Fig. 4. Simulated current distribution of the antenna: (a) without metasurface and (b) with NZIM metasurface superstrate.

3.3 Efficiency, gain and axial ratio

Fig. 5 shows the simulated radiation efficiency of both configurations with and without metasurface . The unloaded patch reaches an efficiency of approximately 69% at 5.8 GHz, whereas the NZIM-loaded antenna reaches about 95% at the same frequency. This enhancement indicates that the metasurface does not introduce excessive losses and that it helps concentrate the radiated field in the useful direction.

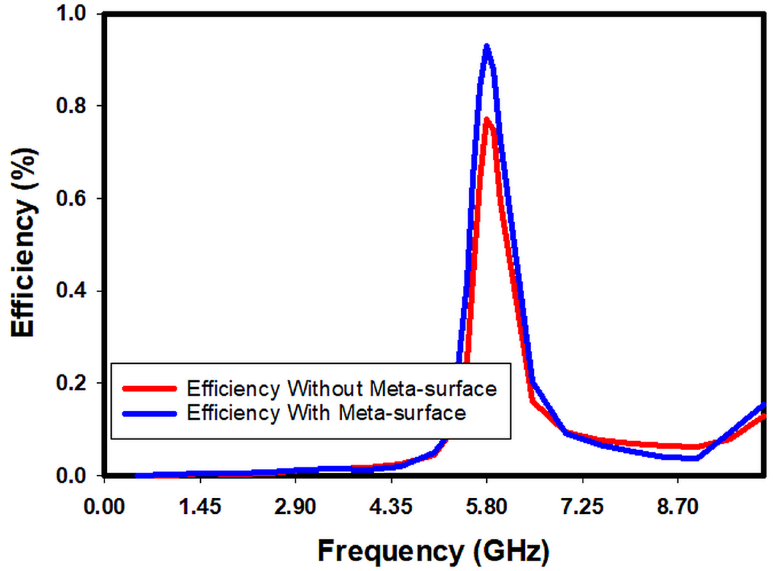

Fig. 5. Simulated radiation efficiency of the proposed antenna with and without the NZIM metasurface superstrate.

The simulated gain is presented in Fig. 6. At 5.8 GHz, the gain increases from 6.1 dBi for the reference antenna to 10.2 dBi for the antenna loaded with the NZIM superstrate. This corresponds to a gain enhancement of about 4.1 dB. This refinement is attributed to the near-zero refractive index of the superstrate, which typiclly reduces phase variations across the aperture and to collimate the radiated beam in the normal direction .

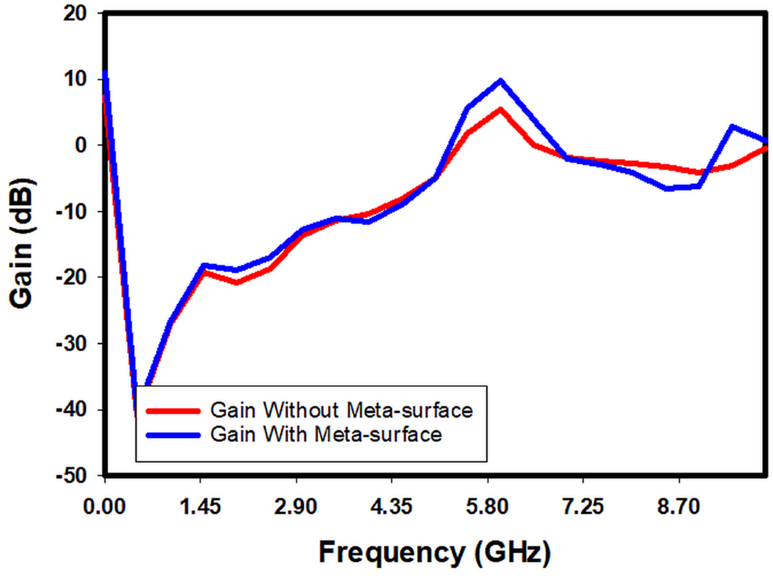

Fig. 6. Simulated gain of the dual-fed square patch antenna with and without the NZIM metasurface superstrate.

Fig. 7 reports the axial-ratio response of the antenna. The standalone dual-fed patch shows an axial ratio close to 12 dB around the operating frequency, which indicates that its polarization is not sufficiently circular without additional loading. When the NZIM superstrate is included, the axial ratio decreases below 3 dB near 5.8 GHz. This confirms that the metasurface contributes to the phase balance between the orthogonal field components and improves the circular polarization behavior.

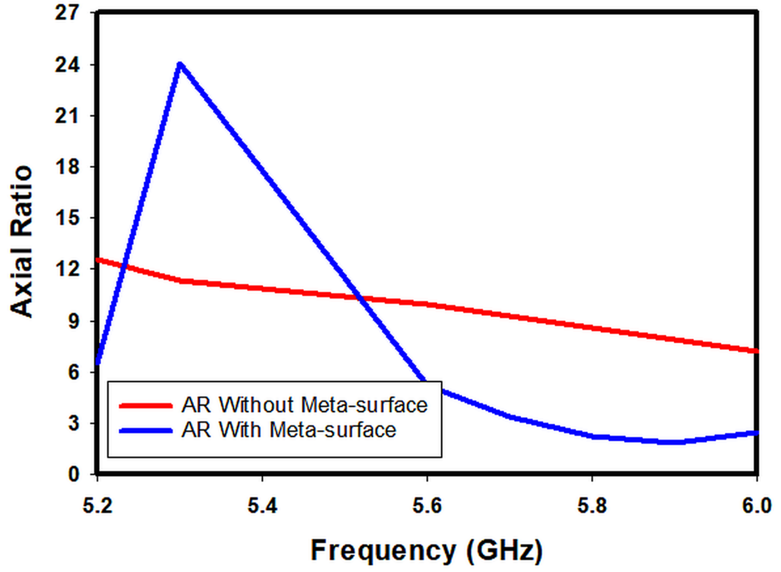

Fig. 7. Simulated axial ratio of the proposed antenna with and without the NZIM metasurface superstrate.

3.4 Radiation patterns

The two-dimensional radiation patterns in Fig. 8 show that the NZIM superstrate reduces the beamwidth and improves the broadside radiation level in both principal planes. This behavior is consistent with the effective near-zero-index response observed in the unit-cell study. The 3D patterns in Fig. 9 further confirm that the metasurface-loaded antenna produces a more concentrated main lobe than the reference antenna.

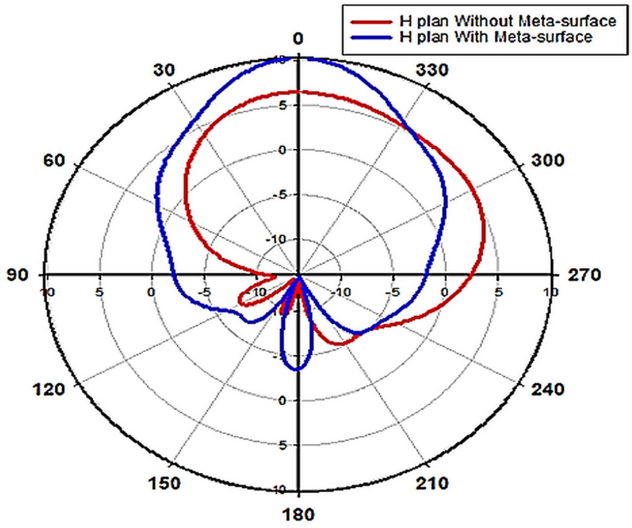

(a)

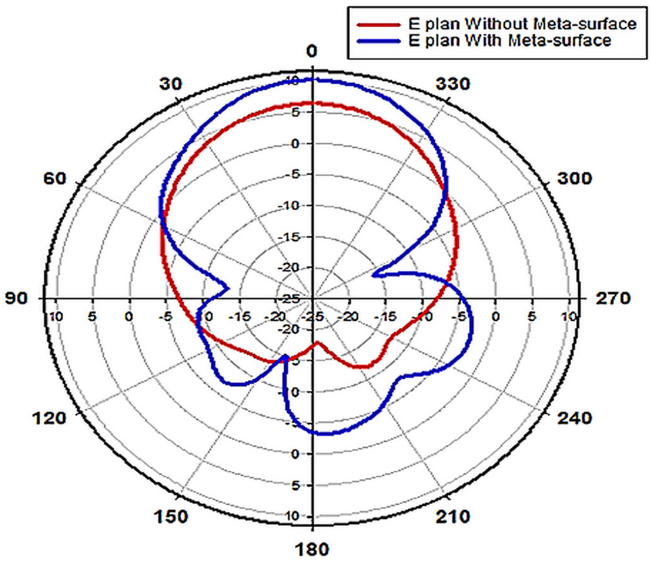

(b)

Fig. 8. Simulated 2D radiation patterns of the proposed antenna: : (a) H-plane pattern with and without metasurface. (b) E-plane pattern with and without metasurface.

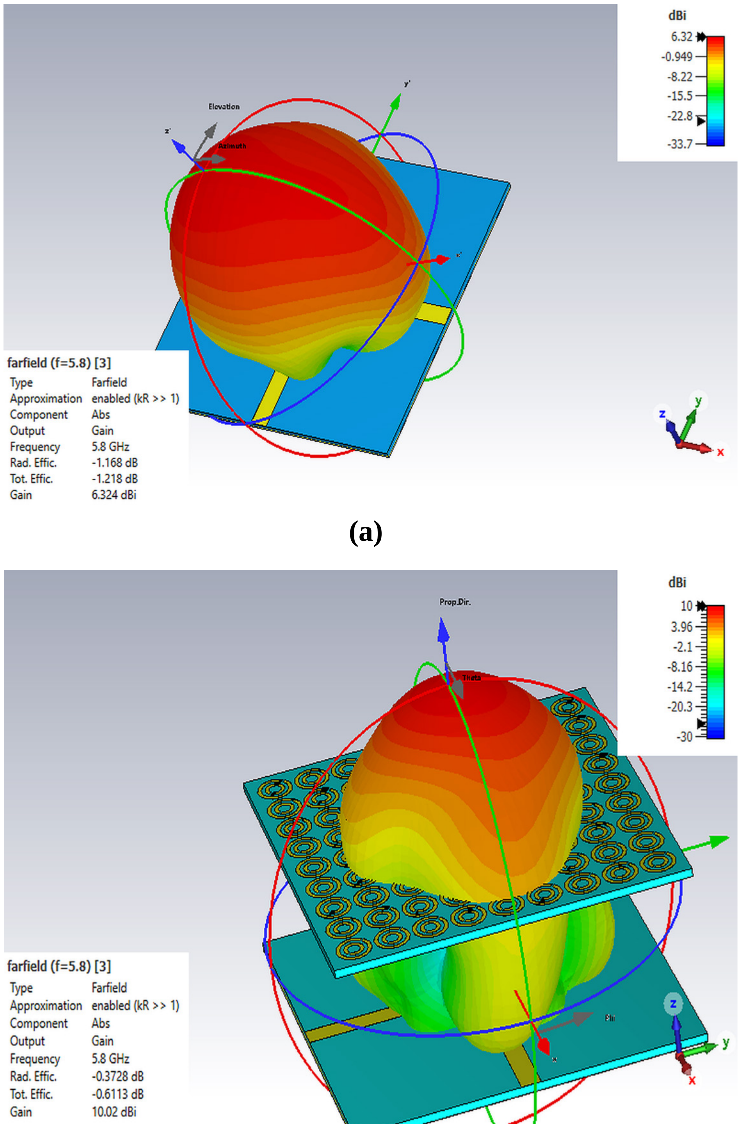

Fig. 9. Simulated 3D radiation pattern of the dual-fed square patch antenna: : (a) without metasurface superstrate.(b) with NZIM metasurface superstrate.

3.5 Overall performance comparison

The main simulated performance indicators are summarized in Table 1. The addition of the NZIM metasurface improves the gain and radiation efficiency while maintaining good impedance matching and inter-port isolation. The axial ratio is reduced below 3 dB, demonstrating that the loaded structure provides a clear improvement in circular polarization compared with the reference antenna.

Table 1. Performance comparison of the dual-fed square patch antenna with and without the NZIM metasurface.

Parameter	Without NZIM metasurface	With NZIM metasurface
Resonant frequency	5.8 GHz	5.8 GHz
Reflection coefficient S11	< -10 dB	< -10 dB
Inter-port isolation S21	> 30 dB near resonance	> 30 dB near resonance
Peak gain	6.1 dBi	10.2 dBi
Axial ratio near 5.8 GHz	about 12 dB	< 3 dB
Radiation efficiency	69%	95%

4 Conclusion

A dual-fed circularly polarized square patch antenna loaded with a single-layer near-zero-index metasurface has been presented for 5.8 GHz wireless applications. The antenna uses two orthogonal quarter-wave feeds to excite the TM10 and TM01 modes, while the NZIM superstrate enhances the radiation performance. The obtained effective parameters confirm a near-zero refractive index around the operating frequency, supporting the physical explanation of beam collimation.

The simulated results show that the metasurface increases the gain from 6.1 dBi to 10.2 dBi and improves radiation efficiency from 69% to 95%. The axial ratio is reduced from 12 dB to below 3 dB near 5.8 GHz, confirming circular polarization. These results demonstrate that a single-layer NZIM superstrate can be an effective solution for compact antennas requiring gain enhancement and polarization reliability.

Future work will focus on fabrication, measurement validation and further bandwidth improvement through alternative metasurface unit-cell geometries.

References

1. S.-L. Chen, D. K. Karmokar, Z. Li, P.-Y. Qin, R. W. Ziolkowski, Y. J. Guo, Circular-polarized substrate-integrated waveguide leaky-wave antenna with wide-angle and consistent-gain continuous beam scanning. IEEE Trans. Antennas Propag. 67, 4418-4428 (2019). https://doi.org/10.1109/TAP.2019.2911398
2. R. B. Waterhouse, Microstrip Patch Antennas: A Designer's Guide (Kluwer Academic Publishers, Boston, 2003)
3. S. J. Chen, C. Fumeaux, Y. Monnai, W. Withayachumnankul, Dual circularly polarized series-fed microstrip patch array with coplanar proximity coupling. IEEE Antennas Wirel. Propag. Lett. 16, 1500-1503 (2017). https://doi.org/10.1109/LAWP.2016.2647227
4. L. Bian, Y.-X. Guo, L. C. Ong, X.-Q. Shi, Wideband circularly polarized patch antenna. IEEE Trans. Antennas Propag. 54, 2682-2686 (2006). https://doi.org/10.1109/TAP.2006.880782
5. S. Mener, R. Gillard, R. Sauleau, C. Cheymol, P. Potier, Unit cell for reflectarrays operating with independent dual circular polarizations. IEEE Antennas Wirel. Propag. Lett. 13, 1176-1179 (2014). https://doi.org/10.1109/LAWP.2014.2330623
6. L. Zhang, X. Lei, F. Xing, J. Wu, Design and analysis of a dual-circular polarization reflectarray, in Proc. IEEE Int. Conf. Ubiquitous Wireless Broadband (ICUWB), 1-4 (2016). https://doi.org/10.1109/ICUWB.2016.7790540
7. F. Z. Khoutar, O. Nayat-Ali, M. Aznabet, O. El Mrabet, A multifunctional patch antenna loaded with near-zero index refraction metamaterial. Prog. Electromagn. Res. M 114, 127-137 (2022). https://doi.org/10.2528/PIERM22092203
8. P. Naseri, M. Riel, Y. Demers, S. V. Hum, A dual-band dual-circularly polarized reflectarray for K/Ka-band space applications. IEEE Trans. Antennas Propag. 68, 4627-4637 (2020). https://doi.org/10.1109/TAP.2020.2972650

9. C. S. Geaney, M. Hosseini, S. V. Hum, Reflectarray antennas for independent dual linear and circular polarization control. IEEE Trans. Antennas Propag. 67, 5908-5918 (2019). https://doi.org/10.1109/TAP.2019.2916596
10. Q. Luo, S. Gao, W. Li, M. Sobhy, I. Bakaimi, C. H. de Groot, B. Hayden, I. M. Reaney, X. Yang, Multibeam dual-circularly polarized reflectarray for connected and autonomous vehicles. IEEE Trans. Veh. Technol. 68, 3574-3585 (2019). https://doi.org/10.1109/TVT.2019.2897218
11. X. Tong, Z. H. Jiang, Y. Li, F. Wu, R. Sauleau, W. Hong, Dual-wideband dual-circularly-polarized shared-aperture reflectarrays with a single functional substrate for K-/Ka-band applications. IEEE Trans. Antennas Propag. 70, 5404-5417 (2022). https://doi.org/10.1109/TAP.2022.3145484
12. X. Zhang, F. Yang, S. Xu, M. Li, Single-layer reflectarray antenna with independent dual-CP beam control. IEEE Antennas Wirel. Propag. Lett. 19, 532-536 (2020). https://doi.org/10.1109/LAWP.2020.2969707
13. S. Zhou, F. Yang, S. Xu, M. Li, A dual-circularly polarized reconfigurable reflectarray antenna with independent beam scanning capability. IEEE Trans. Antennas Propag. 72, 7100-7109 (2024). https://doi.org/10.1109/TAP.2024.3430095
14. D. R. Smith, S. Schultz, P. Markos, C. M. Soukoulis, Determination of effective permittivity and permeability of metamaterials from reflection and transmission coefficients. Phys. Rev. B 65, 195104 (2002). https://doi.org/10.1103/PhysRevB.65.195104
15. H. Chen, L. Ran, J. Huangfu, X. Zhang, K. Chen, T. M. Grzegorczyk, J. A. Kong, Left-handed materials composed of only S-shaped resonators. Phys. Rev. E 70, 057605 (2004). https://doi.org/10.1103/PhysRevE.70.057605